



# Hailstorm Events in the Central Andes of Peru: Insights from Historical Data and Radar Microphysics

Jairo M. Valdivia<sup>1</sup>, David Guizado<sup>1,2</sup>, Elver Villalobos-Puma<sup>2</sup>, José Luis Flores-Rojas<sup>1</sup>, Stephany Callañaupa<sup>2</sup>, and Yamina Silva-Vidal<sup>1</sup>

<sup>1</sup>Instituto Geofísico del Perú (IGP), Lima, Peru

<sup>2</sup>Instituto Nacional de Investigación en Glaciares y Ecosistemas de Montaña (INAIGEM), Lima, Perú

**Correspondence:** Jairo Valdivia, Instituto Geofísico Del Perú, Lima, Peru (valdiviaprado.ing@gmail.com)

**Abstract.** Hailstorms, while fascinating from a meteorological perspective, pose significant risks to communities, agriculture, and infrastructure. In regions such as the Central Andes of Peru, the characteristics and frequency of these extreme weather events remain largely uncharted. This study fills this gap by investigating the historical frequency and vertical structure of hailstorms in this region. We analyzed historical hailstorm records dating back to 1958 alongside four years of observations (2017-2021) from Parsivel2 disdrometer and a cloud profiler radar MIRA35c. Our findings indicate a trend of decreasing hail frequency (-0.5 events/decade). However, the p-value of 0.07 suggests the need for further investigation, particularly in relation to environmental changes and reporting methods. The results show that hailstorms predominantly occur during the austral summer months, with peak frequency in December, and are most common during the afternoon and early evening hours. The analysis of radar variables such as reflectivity, radial velocity, spectral width, and linear depolarization ratio (LDR) reveals distinct vertical profiles for hail events. Two case studies highlight the diversity in the radar measurements of hailstorms, underscoring the complexity of accurate hail detection. This study suggests the necessity for refining the Parsivel2 algorithm and further understanding its classification of hydrometeors. Additionally, the limitations of conventional radar variables for hail detection are discussed, recommending the use of LDR and Doppler spectrum analysis for future research. Our findings lay the groundwork for the development of more efficient hail detection algorithms and improved understanding of hailstorms in the Central Andes of Peru.

## 1 Introduction

Hail is a type of precipitation that forms when strong thunderstorms produce updrafts that carry raindrops high into the atmosphere (Knight, 1981; Knight and Knight, 2001). As the raindrops are lifted higher and higher, they encounter freezing temperatures and become coated with ice. Eventually, these ice-coated raindrops grow to a large enough size and fall to the ground as hail (Knight, 1981). The formation of hail is a complex process that involves several microphysical processes (Pruppacher and Klett, 2010). Storms can produce hailstones from either type of embryo, including heavily rimed snow particles and frozen drops (Knight, 1981). Hailstones grow mainly by collecting supercooled liquid cloud droplets and raindrops within the updrafts of convective storms (Pruppacher and Klett, 2010). These growth processes are further characterized by different



25 growth regimes that describe the physical properties of the resulting hailstones (Ludlam, 1958; Lamb and Verlinde, 2011). Typically, hailstones enter warmer air and partially or completely melt as they fall (Rasmussen and Heymsfield, 1987). When they reach the surface, hailstones exceeding 2 cm in diameter are considered severe (Raupach et al., 2021).

Hailstorms pose a significant threat globally (Allen et al., 2020), leading to extensive damage and substantial financial losses (Púčik et al., 2019; Diaz and Murnane, 2008). In the USA, for instance, these storms result in losses of around US\$10 billion every year (Diaz and Murnane, 2008), with a single severe hail event capable of causing over US\$1 billion in damage (Changnon, 2009; Allen et al., 2017). Areas with high population density are particularly vulnerable, as demonstrated by the 1999 hailstorm in Sydney, Australia, the 2012 hailstorm in Phoenix, Arizona, USA, and the 2013 hailstorms over central and southwest Germany, which caused losses of billions of dollars (Kunz et al., 2018; Allen and Allen, 2016; Allen et al., 2017). Similarly, hailstorms in the Mantaro river valley in Peru, despite being located in a different region, can cause significant damage to crops, property, and infrastructure in the area, especially during the summer season when hailstorms are more prevalent.

In the Mantaro river valley and a large portion of land is owned by small and medium-sized producers who engage in crop diversification as a protective measure against extreme weather and market fluctuations, and climate change (Giráldez et al., 2020, and references therein). Over the years there have been changes in precipitation regimes with a reduction in precipitation trends (-5.6 mm/decade) in the last decade (Giráldez et al., 2020; Silva et al., 2008). Furthermore, anthropogenic climate change is expected to have significant impacts on hailstorms (Raupach et al., 2021), which can result in damaging consequences (Trapp et al., 2019, 2007; Brooks, 2013). The low-level moisture and convective instability (Diffenbaugh et al., 2013; Hoogewind et al., 2017; Rasmussen et al., 2020), melting level height (Dessens et al., 2015; Xie et al., 2008; Prein and Heymsfield, 2020), and vertical wind shear (Weisman and Klemp, 1984; Dennis and Kumjian, 2017) are all expected to change with geographical variability, leading to changes in hailstorm frequency and severity (Mahoney et al., 2012; Brimelow et al., 2017; Kunz et al., 2009). However, due to limited direct observations of hail, incomplete understanding of the microphysical and dynamical processes, and challenges in running models at sufficient resolution, the response of hailstorms to warming remains highly uncertain (Raupach et al., 2021). Despite its potential for damage, little is known about the frequency of hail occurrences in the region. In South America, there are few historical records of hailstorms, and there is no clear general trend in the frequency of these events. Most of these observations are from Argentina, which is one of the regions with the highest likelihood of hailstorms in the region (Prein and Holland, 2018). However, there are regional differences in the trend of hail occurrence. In northern Argentina, there is a positive trend in the frequency of hailstorms, while in the central and eastern regions of Argentina, a negative trend has been observed (Mezher et al., 2012). Beal et al. (2020) observed that on the southern border of Brazil and Argentina there are both positive and negative trends and stations that did not register significant trends. Studies on the effects of climate change on hail are rare in South America (Martins et al., 2017; Beal et al., 2020; Prieto et al., 1999) and there are no references in the literature on future projections of hail or storms over the region.

The global picture of how hailstorms will be affected by climate change in the future remains uncertain, with many regions unstudied, a lack of long-term observational data, gaps in understanding at the process level complicated by interactions



between atmospheric variables relevant to hail, and limited modeling of hail. Consequently, Raupach (Raupach et al., 2021) made five recommendations for future studies:

- 60 – Improved observational records of hail are required, including long and homogeneous data sets to enable separation of natural climate variability from potential trends due to anthropogenic climate change. When possible, observations should include both hail frequency and hailstone size.
- Statistical proxy relationships between environmental conditions and hail occurrence must be evaluated and improved. Proxy studies are extremely valuable, but current relationships typically cannot account for hailstorm initiation. These  
65 statistical links need to be tested in hail-resolving model simulations to detect possible future changes. Alternatively, machine learning approaches that allow for non-stationarity could be considered.
- Process-oriented studies are necessary, including detailed analysis of the microphysical chain of events leading to hail production within the storm and its final impact on the ground. Connections between dynamic processes on the synoptic and climate scales must also be understood. Investigations should focus on low-level moisture and convective instability,  
70 microphysics, and storm initiation. Field experiments and simulations can be used to enhance the understanding of fundamental microphysical processes.
- Changes to hail damage and its economic impact require deeper investigation, with attention not only on hail properties but also on changes to hail exposure and vulnerability. Possible investigation approaches include coupling convection-resolving simulations to impact models and projections of future population growth, and the use of statistical tools that  
75 can deal with non-stationarities in relationships between hazard, exposure, vulnerability and climate change. Future studies should also include modelling of the potential future economic impact of hail.
- More high-resolution numerical model simulations are required to better resolve hailstorm processes and to investigate expected future changes around the globe. As computational power increases, it will be possible to run convection-resolving simulations over larger regions and for longer time periods at increasing resolution and in ensemble modes.

80 In the Andes, apart from studies in the Argentine Andes (Prieto et al., 1999), to date, there are no studies on the climatology or frequency of hailstorms in the Andes. In particular, the lack of quality meteorological data in the Andes has been a major limitation in understanding extreme weather events, such as hail. In this context, the Geophysical Institute of Peru (IGP) has played a fundamental role through the Huancayo Observatory. Aware of the need for quality meteorological data in the region, the IGP has established a set of instruments and sensors at the Huancayo Observatory, in the Laboratory of Atmospheric  
85 Physics and Microphysics and Radiation (LAMAR; (Flores-Rojas et al., 2021)), to study the properties of the atmosphere and clouds, including hail.

In this article, we will explore the climatology and microphysics of hail in the Peruvian Andes, examining the observational features of its formation and the ways in which it can be studied and identified. To better understand the microphysics of hail and its frequency in the region, we will analyze historical reports of hailstorms dating back to 1958, as well as four years



90 of observations using data from LAMAR. We will use the Parsivel2 disdrometer and a cloud profiler radar to identify hail  
events and focus on analyzing microphysical parameters associated with hail. The paper is organized as follows: Section 2 will  
describe the data and methodology, including the historical report of hailstorms and instrument characteristics. In Section 3,  
we will describe the results. The hail climatology and instrumental observations of hail will be described, and a couple of study  
cases will be analyzed in detail. The implications and limitations of our findings will be discussed in Section 4, and finally,  
95 Section 5 will summarize the main findings and conclusions.

## 2 Data and Methodology

This study utilized data collected at IGP's Huancayo Observatory (12°01'18"S, 75°39'22"W), located at 3330 m MSL in  
the central part of the Peruvian Andes. The observatory houses LAMAR, a collection of instruments for atmospheric studies  
(Flores-Rojas et al., 2021), as well as a conventional weather station that has been in operation since 1922. LAMAR is within  
100 the Mantaro valley, which is part of the Mantaro river basin covering some territories of the Ayacucho, Huancavelica, Pasco,  
and Junin regions, surrounds the observatory. The basin has an average altitude of 3870 m asl, with an estimated annual  
precipitation of less than 1600 mm year<sup>-1</sup>. Almost 83% of the annual rainfall occurs during the rainy season, which lasts from  
September to March. The rest of the rainfall occurs during the dry season, which lasts from April to August.

Historical hailstorm reports were collected and digitized for analysis. The information includes the date, time, and in some  
105 cases, the duration of the events, and is recorded daily by the meteorological observer. Data collection was done by Valdivia and  
Silva (2016) for the period of 1958 to 2016. Unfortunately, hailstorms stopped being reported in 2016 due to staff changes. The  
observer only reported hailstorms that were observed over the Huancayo Observatory, which are typically very localized. The  
instruments with advanced technology, such as the optical disdrometer Parsivel2 and the vertically pointing radar MIRA-35c,  
have been installed at the Huancayo Observatory to provide more accurate and comprehensive measurements of hydrometeors,  
110 including hail.

### 2.1 Optical disdrometer Parsivel2

Parsivel2 is the next version of the Parsivel, an laser-optical disdrometer that measure the size and velocity of hydrometeors  
(Löffler-Mang and Joss, 2000). The Parsivel2 has been evaluated through a comparative study at NASA's Goddard Space  
Flight Center (Tokay et al., 2014). The Parsivel2 sampling output is 1 min. The raw data provides the number of drops in  
115 a 32 × 32 size versus velocity matrix. The size range is from 0 to 25 mm, and the class width increases from 0.125 mm in  
small sizes to 3 mm in biggest sizes. The fall velocity range is from 0 to 25 m s<sup>-1</sup>, and the class width increase with the fall  
velocity. The Parsivel2 has been operating since 2017. The internal software computes the rainfall parameters such as rain  
intensity, number of detected particles, particle velocity, and weather code. The Parsivel2 assigns a precipitation classification  
whenever precipitation is observed. The classification is based on the format of precipitation type SYNOP wawa4860 weather  
120 code developed by World Meteorological Organization (WMO). The categories are: Drizzle, drizzle with rain, rain, rain drizzle  
with snow, snow, snow grains, freezing rain, hail. Parsivel2's internal processing filters out very small droplets (less than 0.7



**Table 1.** MIRA35c specifications.

Frequency	34.85 GHz
Peak power	2.5 kW
Receiver	Single Polarization
Operation mode	Pulsed
Beam width	0.6°
Antenna type	Cassegrain
Range resolution	31 m
Temporal resolution	5.6 s
Number of range gates	415
No. of spectral bins	128

mm) that are well above the theoretical droplet velocity. We are not applying any additional post-processing or filtering as our intention in the first instance is to evaluate the entire raw data matrix.

The Parsivel2 disdrometer has several limitations, as evidenced by the findings from various studies. One major limitation is the instrument's sensitivity, which may not be adequate for detecting very small hydrometeors, resulting in underestimation of the total number of particles and their size distribution (Battaglia et al., 2010; Park et al., 2017). Furthermore, the Parsivel2 can struggle to accurately classify irregularly shaped hailstones or complex snowflake shapes, leading to errors in size distribution measurements (Battaglia et al., 2010). The Parsivel2 measures rainfall at a single point, which might not be representative of the overall precipitation in the surrounding area, particularly during convective events with high spatial and temporal variability (Jaffrain et al., 2011; Jaffrain and Berne, 2011, 2012; Tokay et al., 2016; Angulo-Martínez et al., 2018; Jia et al., 2019). Environmental factors, such as wind, temperature, and humidity, can also impact the instrument's performance and the accuracy of its measurements (Friedrich et al., 2013a, b; Park et al., 2017). Several studies have attempted to correct the Parsivel2's measurements to improve their accuracy, such as adjusting the fall velocity of particles (Battaglia et al., 2010; Raupach and Berne, 2015) or investigating the effects of various factors on particle fall velocity (Jia et al., 2019).

Under non-extreme conditions, the Parsivel2 disdrometer demonstrates reliable performance, especially in moderate rainfall ( $R < 10 \text{ mm h}^{-1}$ ) and for midsize drops (0.6 - 4 mm in diameter) (Tokay et al., 2014; Park et al., 2017). At the Huancayo Observatory, comparisons between the Parsivel2 and rain gauges indicate a systematic underestimation of total rainfall (Valdivia et al., 2020b; Kumar et al., 2020; Del Castillo-Velarde et al., 2021). This underestimation bias is around of 16% for a single rainfall event.

## 2.2 Vertically pointing radar MIRA-35c

The MIRA-35c is a high-frequency cloud profiler radar. And it is sensitive to clouds and precipitation. MIRA-35c was manufactured by Meteorologische Messtechnik GmbH (METEK) and operates at a frequency of 34.85 GHz ( $\lambda = 8,6 \text{ mm}$ ), it uses



a magnetron providing 2.5 kW pulse power and transmits a linear polarized signal, while two polarized signals are received simultaneously. The system covers a range between 150 m and 13 km above the ground at a vertical range resolution of 31 m.  
145 Data from the range bins below 250 m are not used because of near-field clutter. The Table 1 shows the complete specifications of this MIRA35c installed at LAMAR. In this work the original software products are used in order to standardize the data. The analysis focuses on the 4 main radar variables, which are:

Reflectivity (dBZe): The equivalent radar reflectivity factor is a measure of the power returned to the radar, which is directly related to the size and number of hydrometeors (raindrops, snowflakes, hailstones, etc.) in the radar's path. High reflectivity  
150 indicates the presence of large or numerous hydrometeors, which often means heavy precipitation. In the context of hail, high reflectivity near the surface could indicate the falling of hailstones.

Radial Velocity: This measures the speed at which the precipitation is moving toward or away from the radar. Since the radar is vertically pointing, the radial velocity is a measure of hydrometeor fall velocity plus the the wind vertical motion. In storms, this can provide information about wind patterns and the movement of the storm itself. High radial velocities may indicate  
155 intense updrafts and downdrafts, which are associated with severe weather conditions such as hailstorms.

Spectral Width (RMS): This is a measure of the variability of the radial velocity within a single radar resolution volume. High spectral width values can indicate turbulence or it can be a measure of how different are the hydrometeors velocity or a combination of both. In severe weather situations like hailstorms, this turbulence can be caused by strong updrafts and downdrafts or by the collision and interaction of different types of hydrometeors.

160 Linear Depolarization Ratio (LDR): This is a measure of the difference in returned power between horizontally and vertically polarized radar signals. It can provide information about the shape and orientation of hydrometeors. Higher LDR values can indicate the presence of non-spherical hydrometeors like hailstones.

### 3 Results

#### 3.1 Historical hailstorms observations over Huancayo Observatory

165 The analysis of historical hailstorm reports focused on the number of events, as data on duration were limited. Although the reports date back to 1958, the first recorded hailstorms appeared in 1962. Figure 1a shows the time series of historical hailstorm reports. A significant number of hailstorms occurred between 1963 and 1976, including the highest number of recorded hailstorms in a single year (1965). The number of reports then declined from 1973 to 1974 and reached zero from 1977 to 1984.

170 A fluctuating cycle of increasing and decreasing events emerged between 1985 and 1993, with the second-highest number of events reported in 1988. No hailstorms were reported in 1994. However, the behavior of hailstorms from 1995 onward significantly differs from previous years, with only 1 to 5 reports per year and minimal variability. The overall average number of annual reports is 3, with 75% of the data (i.e., the third quartile  $Q_3$ ) falling between 0 and 5 reports per year (Figure 1b). Notably, up to 12 events were reported per year in 1965 and 1988. A trend analysis of the data from 1985 reveals a negative  
175 trend of -0.5 hailstorms per decade, with a p-value of 0.0737 (Figure 1a).

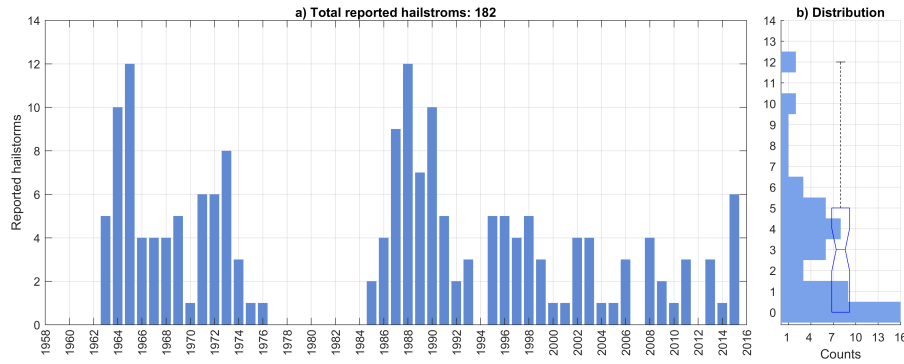


**Figure 1.** a) Historical series of storms reported at the Huancayo Observatory between 1958 and 2016. b) The bars show the histogram of the distribution of reported hailstorms, the same distribution is shown with the box plot.

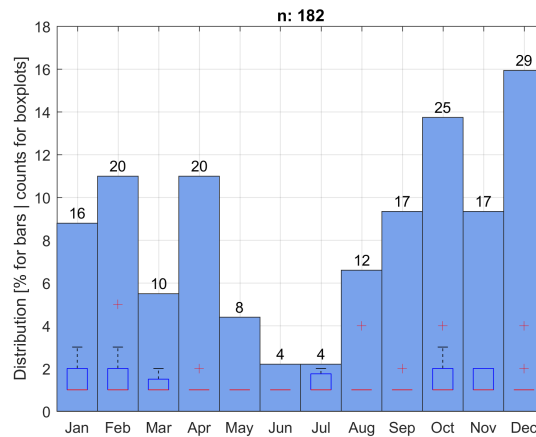


**Figure 2.** Monthly distribution of reported hailstorms, the y-axis shows the relative distribution of all data, while the number above each bar indicates the total number of reports for the month. For each month, the box plot of the annual distribution of hailstorm reports is shown. The total number of reported hailstorms is 182.

Figure 2 shows the monthly distribution of reported hailstorms. The inter annual behavior of the reported hailstorms has a similar behavior that the precipitation cycle (Villalobos-Puma et al., 2019; Kumar et al., 2020; Chavez et al., 2020). The rainy season occurs during Austral summer monsoon (December, January, February and March). From September to November is considered as the transition period. June and July are the driest months of the year and also have the lowest historical incidence of hailstorms. Despite the fact that October and December are the months with the highest reported events, it can be seen in the box plot of Figure 2 that January, February and October show the greatest variability in the number of events reported per year, and that at the same time these are months with a high number of historically reported events. In several of the months, only one event per year has been registered, meaning that any number of events greater than one is considered an outlier (Figure 2).

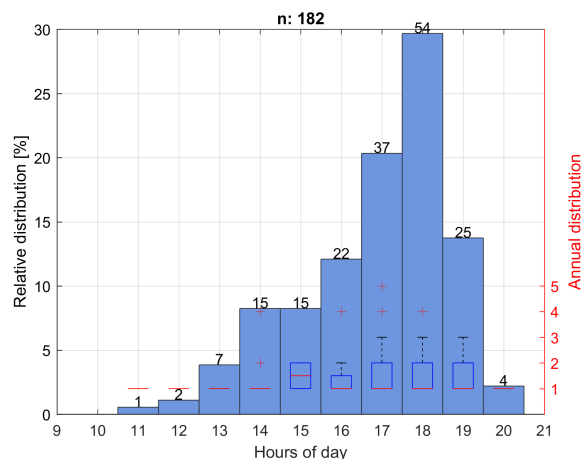


**Figure 3.** Diurnal cycle of reported hailstorms from 1958 to 2016. The y-axis (left) represents the relative distribution of all data, while the number above each bar indicates the total number of cases recorded for that time of day. The y-axis on the right indicates the annual distribution of the records shown in the box plots. The total number of registered events is 182.

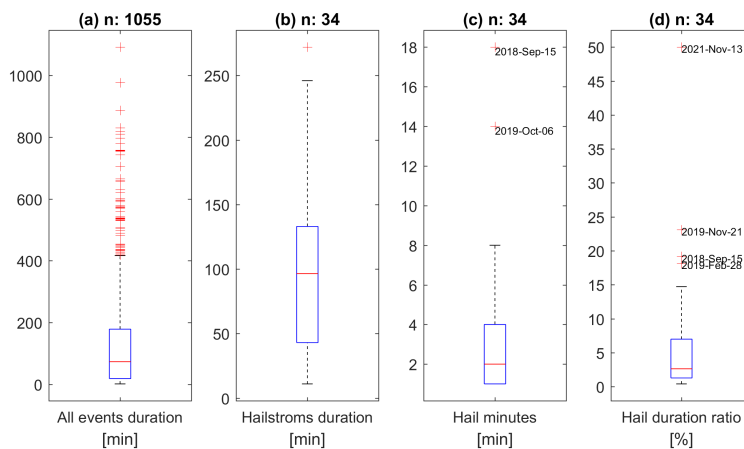


**Figure 4.** Duration distribution of events recorded by Parsivel2. a) Duration of all precipitation events, including liquid and solid. b) Duration of hailstorm events. c) Duration of hail minutes in hailstorms events. d) Relative duration of hail minutes within the event.

Figure 3 shows the diurnal cycle of reported hailstorms. It can be seen that hailstorms are only reported between 11 and 20 hours. Only 3 events have been registered before 13 hours, and almost 20% of events have been registered at 18 hours (54 events). The hours with the greatest annual variability are from 13 to 17 hours, while in other hours only 1 event per year is usually recorded.



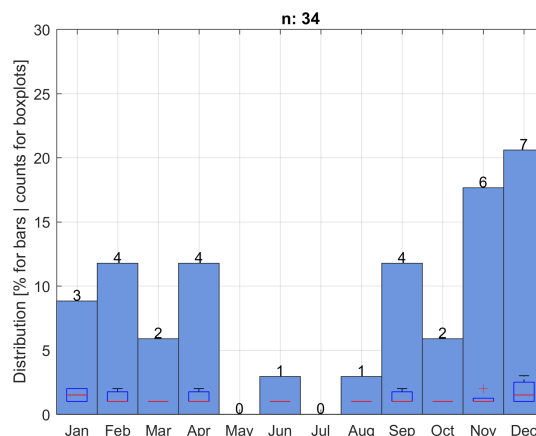


**Figure 5.** Same as Figure 2 but for monthly distribution of hailstorms detected by Parsivel2. The total number of reported hailstorms is 26.

### 3.2 Disdrometer hailstorms observations

The disdrometer allows us to classify all precipitation events. Here we define an event of precipitation following Tokay Tokay et al. (2014) definition. A precipitation event is defined as a period of precipitation separated by 2 hours or longer precipitation-free periods in the rain-rate time series of the disdrometer. Single minute events has been discarded. The rain/no-rain threshold was a set of minimum of 10 drops and a rain rate of  $0.1 \text{ mm h}^{-1}$ . Figure 4 shows the distribution of the duration of the events recorded by the Parsivel2. 1055 precipitation events were found, of which 35 were classified as hailstorm events. Most of the precipitation events are less than 200 min in duration (i.e. between the first and third quartiles,  $Q_1 - Q_3$ ; Figure 4a), however, the whisker in the boxplot reaches 400 min and there are several events above that reach up to 1100 min (Figure 4a). Long duration events in the area are related to stratiform events (Villalobos-Puma et al., 2019) that can last all night. Hailstorms last less than 250 min, half of the events last between 40 and 125 min (i.e. between the first and third quartiles,  $Q_1 - Q_3$ ; Figure 4b). Hailstorm events in the area are usually mixed with rain, among the 34 registered hail events, 75% events have 1 to 4 min of hail and two events were found whose duration is 14, and 18 min, respectively. They appear as outliers in the boxplot of Figure 4c. In relative terms, the minutes of hail do not exceed 7% of the total event duration in the 75% of the events (i.e. the second quartile is 7%; Figure 4d). There are four events where the hailstorm minutes are above normal, with 18%, 19%, 23%, and 50% of the duration of the event, respectively.

Despite the fact that the observation period of the disdrometer is only from 2017 to 2021, very short to establish a climatology, it is important to see if the behavior of the events is similar to that of the historical reports. Figure 5 shows the monthly distribution of hailstorms detected by Parsivel2. No events were recorded between the months of May and July, which coincides with the dry season and the few events recorded in historical reports. Most months have too few events recorded to be considered statistically relevant. An increase is observed in the month of September, which would be linked to the transition period. November and December are the months with the highest number of events detected. As in the historical records, the

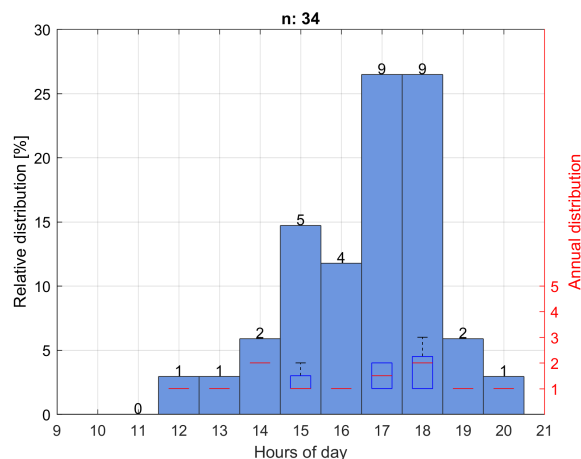


**Figure 6.** Same as Figure 3 but for diurnal cycle of hailstorms detected by Parsivel2. The total number of reported hailstorms is 26.

month of April has a higher number of hail events. The box plots in Figure 5 do not give much information since in most months there is only one event recorded. Figure 6 shows the diurnal cycle of hailstorms measured by Parsivel2. The hours in which the events occur are the similar as those reported historically. Hailstorms are only reported between 13 and 20 hours. Only 1 event have been measured at 13 hours, and and all other events after 15 hours. 30% of events have been registered at 17 hours (8 events). The hours with the greatest annual variability are from 15, 17 and 18 hours, while in other hours only 1 event per year was recorded.

### 215 3.2.1 Microphysical characteristics of hail

The types of precipitation recorded by the Parsivel2 have been classified according to the Synop code wawa4860 (WMO). The categories include drizzle, drizzle with rain, rain, rain drizzle with snow, snow, snow grains, freezing rain, and hail. Figure 7 shows a histogram of the occurrence of different types of precipitation for the one-minute resolution Parsivel2 recording. The most common types of precipitation at the Huancayo Observatory are rain, drizzle with rain, and drizzle, accounting for 220 55.73%, 38.78%, and 5.35% of events, respectively. This suggests that the majority of precipitation at the observatory is in the form of rain or light drizzle. Only 1.4% of events are from the other categories, with hail representing a very low 0.09%. It is worth noting that the minutes of hail in the study area are significantly lower compared to the amount of rain recorded. This is evident in the histogram of Figure 7, where the number of hail events is much smaller than the number of rain events.

Figure 8 shows the relationship between the terminal velocity and the diameter of the particles observed by Parsivel2 for the minutes classified as hail. A total of 66 minutes of hail were identified in the period from 2017 to 2021. The size-velocity matrix and hail size distribution measured with Parsivel2 indicate that hailstones in the area do not usually exceed 14 mm in diameter and they can reach 21 m<sup>-1</sup>. One particle was measured between 14 mm and 16 mm, with less than 1 m<sup>-1</sup>. Despite the fact that only minutes of hail are shown, it can be seen in Figure 8 that there are also a large number of raindrops present,

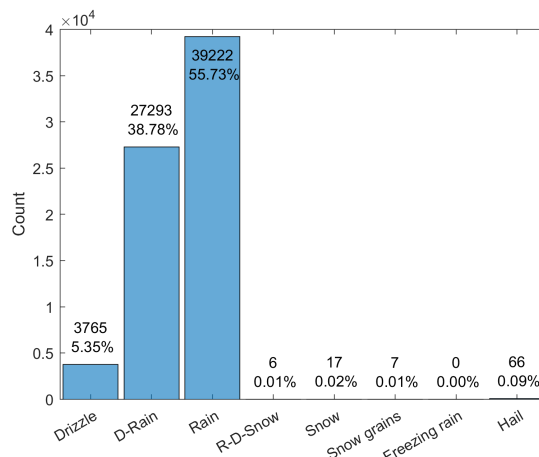


**Figure 7.** Types of precipitation recorded by Parsivel2 according to the Synop code. The y-axis indicates the number of minutes recorded in the entire study period. Above each bar is shown the value of each bar and its relative value.

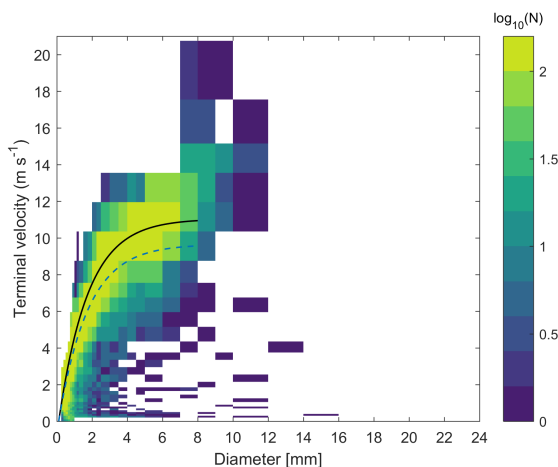


**Figure 8.** Terminal fall velocity as a function of diameter observed by Parsivel2 for the minutes classified as hail (66 min). The theoretical fall velocity for raindrops at 3300 m above sea level is represented by the black line, while the calculation at sea level is depicted by the blue dashed line. It should be noted that this data, while only representing hail minutes, also contains a significant number of raindrops.

230 which follow the theoretical curve of their terminal velocity vs. diameter quite well. It can be difficult to distinguish with the naked eye which data points within the velocity matrix correspond exclusively to hail. No evident hail size-velocity relationship has found. However, we know that raindrops do not usually exceed 8 mm in diameter because they break, nor do they reach very high velocities (Matthews and Mason, 1964; Blanchard and Spencer, 1970; Villermaux and Bossa, 2009). The drops at the Huancayo observatory do not usually exceed 12 m s<sup>-1</sup> (Valdivia et al., 2020b). From this, we can infer that the block of particles observed between 8 and 12 mm in diameter and with velocities greater than 10 m s<sup>-1</sup> may correspond to hail. There

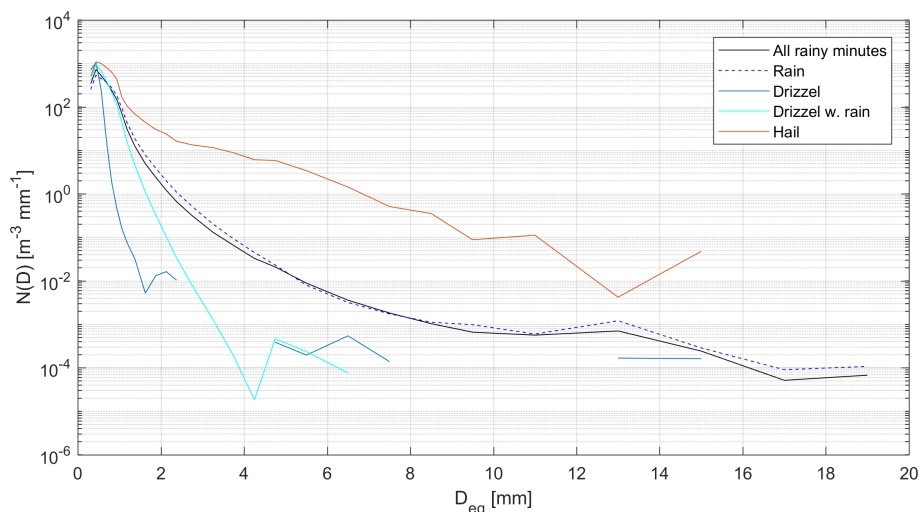


**Figure 9.** Mean particle size distribution for different precipitation types measured by Parsivel2. The black line represents all rainy minutes (124454 min), the dashed blue line represents rain (70548 min), the sky blue line represents drizzle (6782 min), the cyan line represents drizzle with rain (46955 min), and the red line represents hail minutes (66 min).

235 are also several particles that are quite outside the typical raindrop distribution and below the theoretical ratio. It is difficult to say for sure if these data points correspond to hail, but it is definitely not normal behavior for raindrops. Valdivia Valdivia et al. (2020b) conducted an evaluation of the characteristics of the raindrop terminal fall velocity and drop size diameter relationship during a rainy season. Among their findings, it was observed that raindrops are usually distributed quite uniformly close to the theoretical relationship (shown as the black line in Figure 8).

240 The size distribution of hydrometeors for different types is presented in Figure 9. A noticeable difference is observed between the distribution of liquid rain and hail. For hydrometeors larger than 1 mm, the concentration is higher in hail compared to liquid rain. Hail of up to 15 mm was observed, but the average profile of all the data (represented by the black line in Figure 9) shows particles up to 19 mm. Since 56.7% of the data is classified as rain, its distribution closely resembles the combined distribution of all hydrometeor types. The observed larger particle sizes, which are theoretically improbable for raindrops, might be due to  
 245 multiple smaller raindrops passing through the Parsivel2's measurement beam simultaneously or high wind velocities, leading to an overestimation of the particle size. This apparently does not generate an artificial classification as hail. The observation of large particles classified as "rain" when it is theoretically improbable for raindrops to be so large may be explained by the work of Friedrich Friedrich et al. (2013b). Their study suggests that particles with sizes >5 mm and real velocities <1 ms<sup>-1</sup> can be caused by strong winds and splashes on the head of the instrument, which might result in the overestimation of particle  
 250 size. The same phenomenon is observed in the size distributions of drizzle and drizzle with rain, where there is an anomalous increase in the largest sizes of each distribution.



### 3.3 Vertically pointing radar observations

We conducted a statistical analysis of hail events observed by the MIRA35c radar, analyzing their vertical profiles. To compare the characteristics of hail-only minutes to those of the entire event, we separated the hail profiles using Parsivel2, and the comparison is shown in Figure 10. We observed that the reflectivity profiles of hail minutes had slightly higher values near the surface but rapidly fell as the height increased (Figure 10a). This was primarily due to the attenuation generated by hail and the high intensity of rainfall associated with hail events, as discussed in (Bringi and Chandrasekar, 2001; Peters et al., 2010). It is important to note that we did not apply any attenuation correction algorithm in our analysis. In terms of radial velocity (Figure 10b), which is also the falling velocity as the radar points vertically, we noted a notable concentration of velocities around  $10 \text{ m s}^{-1}$ , which exceeded  $12 \text{ m s}^{-1}$ , surpassing the Doppler Nyquist velocity and resulting in aliasing (Doviak et al., 1979). Unlike the distribution of the entire events, the vertical hail profiles slowly lose velocity with height. At a range of 2 km, it is highly unlikely that aliasing will occur in the falling velocities in the absence of hailstones. The hailstone profiles only show velocities approaching  $0 \text{ m s}^{-1}$  above the 4 km range. In contrast, for complete events, this occurs before 2 km, where the bright band of the radar or melting layer is approximately located.

In terms of spectral width (Figure 10c), values below the melting layer had a very similar behavior, with the most frequent values around  $1 \text{ m s}^{-1}$  in both hail-only profiles and the entire event. However, for hail-only profiles, the spectrum was wider towards positive values. Above the melting layer, there was a notable difference in spectral width values, as values in hail minutes did not decrease and tended to increase with height due to turbulence caused by convection in the middle and upper parts of the storm. In the all-event profiles, the mode clusters around  $0 \text{ m s}^{-1}$ , representing the largest amount of data. However, in the hail-only profiles, the mode tends to remain near  $1 \text{ m s}^{-1}$ .

Regarding the linear depolarization ratio (LDR) of the MIRA35c (Figure 10d), there were significant differences in hail-only profiles. The entire vertical profile of LDR shifted to the right. The LDR for the entire event was around -30 dB near the surface, increasing to values around -28 dB above the melting layer with a slightly wider distribution. For hail-only profiles, the behavior was the same, but approximately 5 dB higher, with differences only in the melting layer where LDR values were lower for hail-only. It is important to note that LDR values are higher in the presence of non-spherical particles, so the melting layer presents high LDR values. Raindrops are expected to have lower LDR values than hail. However, our results show that the LDR of the hail tends to be lower than that of the melting layer. This may be because hailstones are usually accompanied by raindrops, decreasing the total LDR, and the turbulence associated with hailstorm processes typically disrupts the melt layer (Houze, 1993; Williams et al., 1995).

### 3.4 Study cases

To analyze the details of how hail events evolve, we selected two study cases. The first case study (E1) occurred on April 10th, 2019, and all the radar variables showed high values, indicating an event of hail (Figure 11). The Parsivel2 data showed that the hailstones fell for approximately 6 minutes around 14:40 LT, a few minutes after the start of the rain. The total duration of the event was approximately 35 minutes. The first 15 minutes of the event presented convective characteristics with high

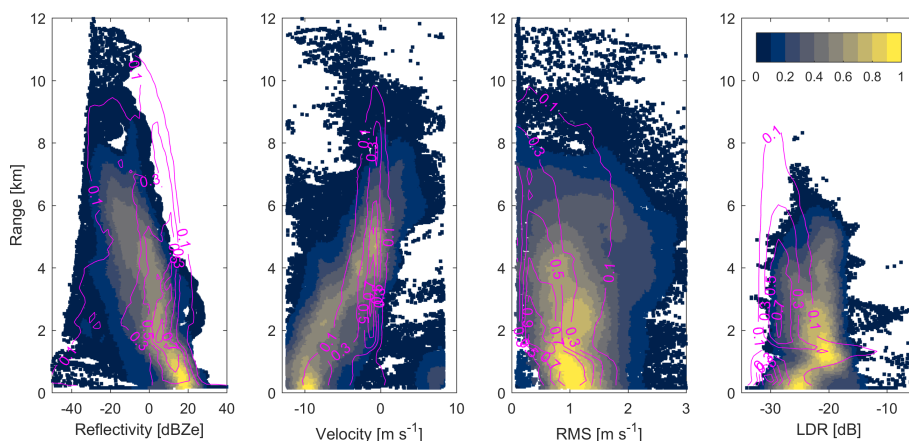


**Figure 10.** Normalized distribution of hail vertical profiles obtained from the MIRA35c radar. The shading colors highlight the profiles flagged as hail in Parsivel2 disdrometer, while the contour lines display the normalized distribution of all hailstorm vertical profiles. The four radar variables (a) equivalent radar reflectivity factor [dBZe], (b) radial velocity [ $\text{m s}^{-1}$ ], (c) spectral width [ $\text{m s}^{-1}$ ], and (d) linear polarization ratio [dB] are shown.

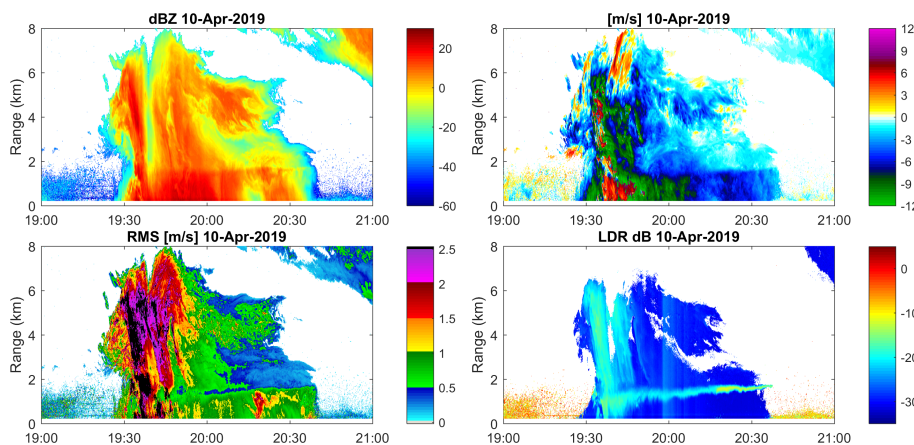


**Figure 11.** Radar variables measured by MIRA35c for Study Case E1 on April 10th, 2019. (a) Equivalent radar reflectivity factor [dBZe], (b) radial velocity [m/s], (c) spectral width [m/s], and (d) linear depolarization ratio LDR [dB] are shown.

285 rain intensity, which then evolved into a stratiform precipitation. Within these first 15 minutes of E1, Parsivel2 classified the precipitation peaks as hail (Figure 12a), with particle diameters greater than 6 mm (Figure 12b). High values of reflectivity and attenuation were observed in Figure 11a, especially during the minutes of hail. The fall velocity during the minutes of hail was quite high throughout the vertical profile (Figure 11b), with downward velocities of  $12 \text{ m s}^{-1}$  from 6 km above the radar to the surface, surpassing the Doppler Nyquist velocity in several sections. As velocities are so high, it is possible that part of the  
 290 Doppler spectrum is constantly surpassing the Doppler Nyquist velocity during the minutes of hail, causing the spectral width



to have altered values due to aliasing, resulting in high values (Figure 11c). Based on the distribution presented in Figure 10c, we can infer that spectral width values above  $2.5 \text{ m s}^{-1}$  could be presented as outliers. These results should be taken into account when developing a hail detection algorithm. The observations indicate that it is imperative to carry out a correct de-aliasing treatment. Under the circumstances presented, it is possible to say that there are velocities much higher than what  
295 would be seen in only liquid rain. The LDR values during the minutes of hail presented values around -20 dB (Figure 11d), which is coherent with the distributions presented in Figure 10d in the presence of hail. It is interesting to note that the high LDR values are shown from a high altitude, covering practically the entire vertical profile of precipitation. Considering that the fall velocities are also high at high altitude, it can be inferred that hailstones are present even above 6 km from the radar. It is possible that the convective system is much larger, and due to attenuation, the radar cannot observe it.

300 The second case study, E2, occurred on March 7th, 2019 (Figure 13). Unlike E1, there were no evident values in the MIRA35c radar variables suggesting that we were in a hail event. However, the Parsivel2 data shows that there were a few minutes of hail just before 14:30 LT (Figure 14a). In the Parsivel2 drop size distribution (Figure 14b), there are no notably larger drops, only a few minutes exceeded 6 mm in diameter, but not exceeding 8 mm. E1 was observed as a convective precipitation of approximately an hour in duration. The convective part occurred in the first 30 minutes of the event, and then  
305 it transformed into a more stratiform rainfall. Near 14:30 LT, when hail was recorded, attenuation in radar reflectivity was observed (Figure 13a). The radial velocity was quite high during the convective minutes, even exceeding the Doppler Nyquist velocity, reaching up to  $12 \text{ m s}^{-1}$  (Figure 13b). Although hail was recorded in the first few minutes of the event, the spectral width appears to be quite homogeneous, with small groups disintegrated between 2 and 4 km, with values between  $1.5 \text{ m s}^{-1}$  and  $2 \text{ m s}^{-1}$  observed at the beginning of the event. Such values are typical in the presence of raindrops. However, below 2  
310 km, the spectral width values are much more homogeneous (Figure 13c), between  $0.5 \text{ m s}^{-1}$  and  $1 \text{ m s}^{-1}$ , which correspond to more typical values of light rain or cloud values (Figure 10c). These observations of uniform spectral width and high fall velocities suggest an absence of turbulence and hail and raindrop sizes quite similar. The LDR values in this part of the event show values close to 20 dB (Figure 13d), which is consistent with the presence of hail, based on the observations of the variable distribution shown in Figure 10d. When the convective system begins to become more stratiform, that is when upward velocities  
315 and high turbulence are observed (Figure 13b,c). Intuition would lead us to think that in these conditions hailstones would only begin to form. However, the LDR values show that hail formation starts much earlier. These results highlight how unreliable conventional variables such as reflectivity, velocity, and spectral width can be for some hail events. In both case studies it can be observed that the duration of high LDR values is greater than the period that Parsivel2 classifies as hail. Probably because hailstones melt quickly near the surface or Parsivel2 is underestimating hail duration.

#### 320 4 Discussion

The present study aimed to analyze the characteristics of hailstorms in a specific region using both ground-based and radar measurements. The analysis showed a decrease in the frequency of hailstorms over time ( $-0.5/\text{decade}$ ), while this trend may not be statistically significant, it is close to the threshold and thus warrants further investigation. It is also unclear whether this



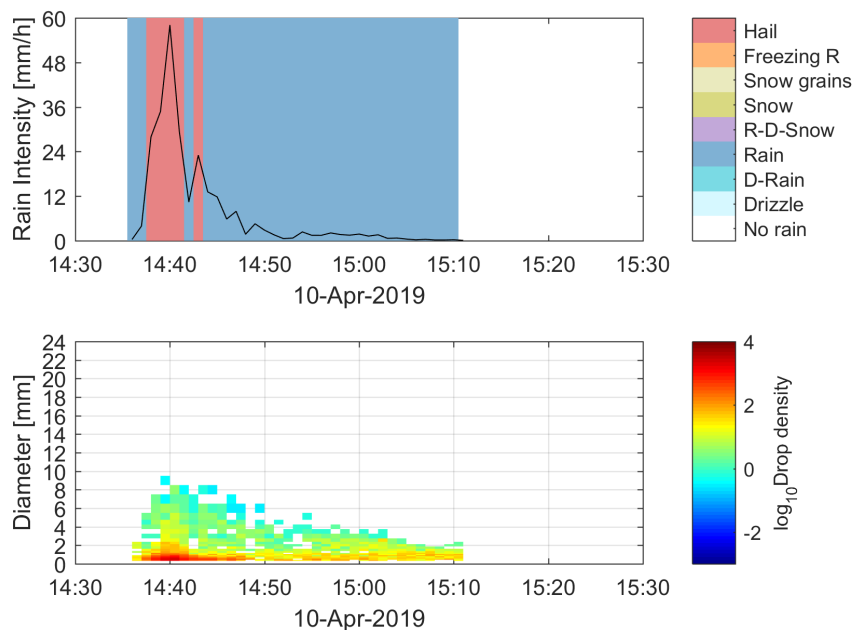


**Figure 12.** Parsivel2 observations for Study Case E1 on April 10th, 2019. (a) shows the rain intensity [mm/h] is shown in black lines along with the Synop 4680 hydrometeor classification in shading color, and (b) shows the hydrometeor size distribution [ $\text{m}^{-1} \text{mm}^{-1}$ ].

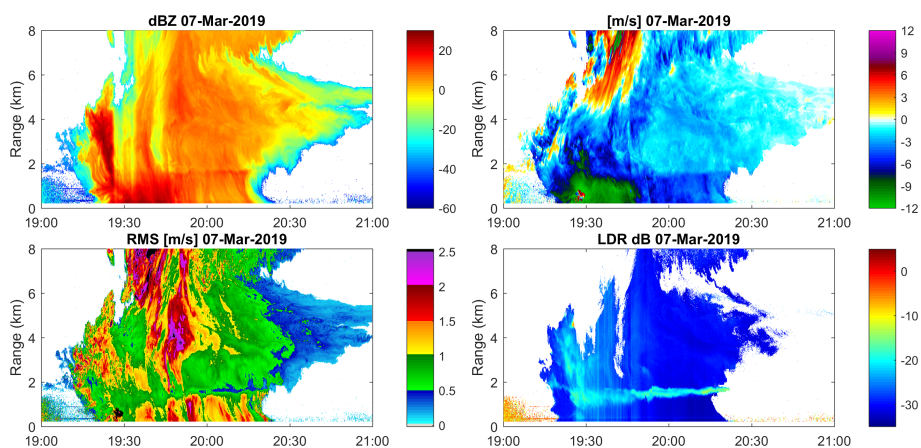


**Figure 13.** Same as Figure 11, but for E2 of March 07th, 2019.

325 trend is due to climate change or changes in reporting methods. Changes in the way hail is reported could lead to errors in these results. On the other hand, negative trends in the frequency of hailstorms between Argentina and Brazil (Beal et al., 2020) are associated with an increase in the melting layer, which in turn is linked to global warming (Xie et al., 2008). Further studies are necessary to determine whether there have been any changes that could lead to a negative trend in hailstorm frequency.



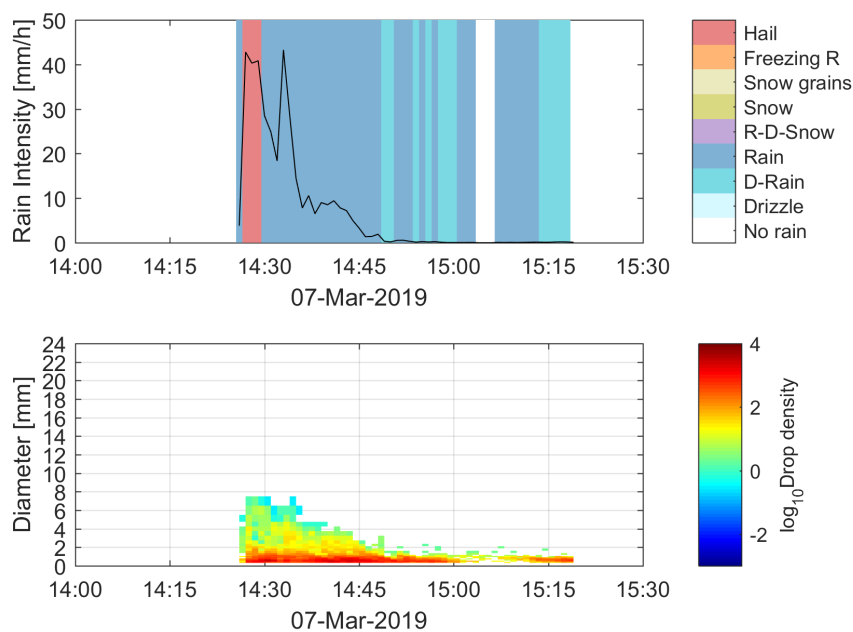


**Figure 14.** Same as Figure 12, but for E2 of March 07th, 2019.

Microphysically, the study found few differences that could be used to identify hail particles. Most particles in the main distribution of drops in the velocity versus diameter matrix were easily counted and were very close to or equal to one. The PSD showed in Figure 9 is evidence that the Parsivel2 classification of hydrometeors is not perfect. One of the most concerning details is that the largest particle sizes recorded by the Parsivel2 correspond to "rain" precipitation, as seen in Figure 9. The DSDs that correspond to liquid rain have droplet diameters that physically should not exist. This error could be evidence of multiple drops traversing the beam simultaneously or hail being marked as rain. In the case of the estimation of microphysical properties in rain. Friedrich Friedrich et al. (2013b) suggests that particles with sizes  $>5$  mm and real velocities  $<1$   $\text{ms}^{-1}$  can be caused by strong winds and splashes on the head of the instrument, which might result in the overestimation of particle size. In our study, it is possible that similar conditions have led to the presence of large particles classified as rain in the Parsivel2 dataset. To account for this, future research could consider implementing additional measures to mitigate the impact of wind-induced splashes or improve the classification algorithm's ability to distinguish between true raindrops and other sources of large particles. Studies focused on the estimation of liquid precipitation suggest applying certain filters to correct the Parsivel2 data, however, in this work no filter was applied due to interest in studying the complete velocity-diameter matrix. It is also important to note that the definition of hail used by meteorological observers may differ from the technical definition of hail, which is defined as ice pellets greater than 5 mm in diameter (WMO, 2017). The present study did not discriminate based on size, instead focusing on how the Parsivel2 algorithm classified the hydrometeors. This Parsivel2's classification method is not well-documented and may lead to errors.



345 The detection of hail using radar variables has proven to be challenging. The reflectivity parameter experiences a rapid decay in the presence of intense precipitation and hailstorms. Additionally, the Nyquist velocity places a constraint on the radial velocity parameter, which poses a significant inconvenience when trying to detect hail. The Nyquist effect also impacts the spectral width parameter, generating artificially inflated values. The linear depolarization ratio (LDR) stands out as the most reliable indicator of hail. However, observations in this work suggest that hail is typically accompanied by raindrops, and  
350 at times, precipitation of rain may dominate the LDR parameter. To study hailstones accurately, the most effective approach is to analyze the Doppler spectrum directly. Multiple peak processing to Doppler velocity spectra (e.g. Williams et al. (2018)) during storms seems to be a nice way to study hail microphysics. However, the Doppler spectrum is typically computationally intensive and requires detailed event-by-event analysis, an aspect left for future study.

The examination of case studies has revealed that hail events exhibit significant variability in terms of radar parameters.  
355 Moreover, failure to attend to the linear depolarization ratio (LDR) parameter could result in the oversight of a hail event. The duration of the LDR parameter during these events raises concerns that Parsivel2 may underestimate the duration of hail events in minutes or that hailstones are melting rapidly near the surface. These details warrant further investigation and will be the subject of future research.

## 5 Summary and conclusions

360 This study aimed to investigate the climatological characteristics of hail events in the Central Andes of Peru. The research utilized historical data from hailstorm records dating back to 1958, as well as four years of observations using Parsivel2 disdrometer and a cloud profiler radar. The focus was on understanding the microphysics of hail and identifying which radar microphysics are associated with hail. We found evidence of a trend in decrease hail frequency (-0.5 events/decade, with the p-value of 0.07 suggest that the observed trend may not be statistically significant, but it is close to the threshold and warrants  
365 further investigation). It is not clear if the trends are the product of environmental aspects such as the increase in the melting layer (Beal et al., 2020; Xie et al., 2008), or if they are human errors induced by changes in the way hail is reported. Such findings need to be evaluated in more detail, aspects regards to environmental changes are important to fully understand trends in hail frequency.

We use the Parsivel2 to classify the types of hydrometeors in the period from 2017 to 2021. Parsivel2 classifies hydrometeors  
370 using the weather code SYNOP wawa4860. The internal Parsivel2 algorithm of classification is not documented. The results for both, the historical report and Parsivel2, showed that hail events in the region are most common during the austral summer months, with a peak in December. Hailstorms tend to occur during the afternoon and evening hours, with a duration of hail-only minutes is most of cases less than 4 minutes. All reported hail events occurred between 10 am and 9 pm LT, and the average number of reported hailstorms is 3 per year. However, Parsivel2 only flagged as hail the 0.12% of the whole dataset. The size-  
375 velocity matrix and hail size distribution measured with Parsivel2 indicate that hailstones in the area do not usually exceed 14 mm in diameter and the can reach  $20 \text{ m s}^{-1}$ . Hail usually falls with raindrops, which is predominant in the diameter-velocity matrix. The conditions that determine the size of the hailstones are still unknown, although we found evidence of a decrease



in the frequency of hailstorms, more research is necessary to know how the size of hailstones will change in the future. Note that increasing their size would imply that they would be more destructive than they already are. Understanding these hailstone characteristics set the stage for a deeper radar-based analysis of hailstorms.

A vertically pointing radar is used to study hailstorm characteristic and four variables are used: reflectivity, velocity, spectral width, and LDR (see Section 2.2). The study shows that hail events have distinct vertical profiles in terms of reflectivity, radial velocity, spectral width, and linear depolarization ratio. The hail profiles have higher reflectivity values near the surface, high falling velocities, and wide spectral width values above the melting layer, indicating turbulence caused by convection in the middle and upper parts of the storm. The linear depolarization ratio of hail-only profiles is also higher than that of the entire events, indicating that hailstones are present even above 6 km from the radar, which means above of 9.3 km ASL. This suggests that deep convection plays an important role in the formation of hail in the Andes.

Two case studies were analyzed in detail. Both cases of hailstorm present very different values in the radar variables, and show how diverse hail can be in terms of radar measurements. The first case study showed high values of reflectivity and attenuation, especially during the minutes of hail. The fall velocity during the minutes of hail was quite high throughout the vertical profile, with downward velocities of  $12 \text{ m s}^{-1}$  from 6 km above the radar to the surface, surpassing the Doppler Nyquist velocity in several sections. The second case study did not show any evident values suggesting a hail event, but the Parsivel2 data showed a few minutes of hail, which could be confirmed through the radar LDR. The homogeneous spectral width of the second event means that hail can occur under low turbulence and a very uniform hydrometeors velocities. These findings highlight the complexity and variability of hail events, which makes them challenging to detect and study.

Future work should focus on reviewing the Parsivel2 algorithm and addressing the issues with the radar's Nyquist velocity and attenuation. Furthermore, determining the specific conditions under which the Parsivel2 misclassifies or overestimates hydrometeors sizes is necessary to improve its performance. Our results suggest that conventional radar variables (reflectivity, velocity and spectral width) are unreliable for correct hail detection. The LDR seems to be the best tool to detect hail with the radar, however, in the area hail is often mixed with raindrops, which can result in quite confusing LDR values. The authors' suggestion to study hail events is to work on the Doppler spectrum, first correcting the aliasing. Separating the spectrum into multiple peaks (e.g. Williams (Williams et al., 2018)) may be the best way to reduce the influence of raindrops on the hail signal. These improvements could significantly enhance our ability to detect and study hailstorms in the Andes and other regions.

In conclusion, our pioneering analysis of hailstorms in the Central Andes of Peru has not only deepened our understanding on microphysics and climatology of hail, but also carved out a path for the development of more effective hail detection algorithms. The implications of this kind of research are far-reaching, ranging from improving weather forecasting and risk management to advancing our understanding of the impacts of climate change. Despite the important strides we have made, the intricate nature of hailstorms leaves much to be discovered. As we continue to refine our methodologies and tools, we hope to learn even more about these intricate weather phenomena, this knowledge promises to bring immense benefits to the communities directly affected by these weather events and to open new horizons for scientific discovery and practical applications. This is just the



beginning of our journey to understand hailstorms in the Andes, and the road ahead is filled with potential for groundbreaking research and innovations.

415 *Data availability.* The data used in this work can be acquired upon request in case of historical report and radar, or download from the repository in the case of Parsivel2 (Valdivia et al., 2020a): <https://www.igp.gob.pe/programas-de-investigacion/ciencias-de-la-atmosfera-e-hidrosfera/facilidad/microfisica/acceso-a-datos>

420 *Author contributions.* J.M.V., D.G., E.V.P., J.L.F.R., S.C., and Y.S.V. conceptualized the study. D.G., E.V.P., S.C., and Y.S.V. provided the resources. J.M.V. and D.G. conducted the formal analysis. J.M.V. developed the software and visualization. S.C. and Y.S.V. secured the funding and administered the project. J.L.F.R. and Y.S.V. supervised the project. J.L.F.R., S.C., and Y.S.V. carried out the investigation. D.G., E.V.P., S.C., and Y.S.V. validated the results. J.M.V. wrote the original draft of the manuscript. D.G., E.V.P., J.L.F.R., S.C., and Y.S.V. reviewed and edited the manuscript.

*Competing interests.* The authors declare that they do not have conflict of interest.

425 *Acknowledgements.* Special thanks to Mr. Gaudencio, who was for many years the meteorological observer at the Huancayo Observatory, his work made this research possible. This work was done under the project "TAMYA - *Impactos de la precipitación, registrados con un radar meteorológico, en los cuerpos glaciares Andinos: nevado Huaytapallana*, CONCYTEC - 082-2021-FONDECYT". We also want to thank to: Gobierno Regional de Junín and Oficina desconcentrada de la región centro de Lima - INAIGEM. We acknowledge the use of OpenAI's GPT, an artificial intelligence language model, during the drafting of this manuscript. Its assistance was primarily utilized for helping with language structure, and enhancing the overall quality and clarity of the text. However, the final interpretations and conclusions presented in this manuscript are solely those of the authors.



## 430 References

- Allen, J. T. and Allen, E. R.: A review of severe thunderstorms in Australia, *Atmospheric Research*, 178-179, 347–366, <https://doi.org/10.1016/j.atmosres.2016.03.011>, 2016.
- Allen, J. T., Tippett, M. K., Kaheil, Y., Sobel, A. H., Lepore, C., Nong, S., and Muehlbauer, A.: An Extreme Value Model for U.S. Hail Size, *Monthly Weather Review*, 145, 4501–4519, <https://doi.org/10.1175/MWR-D-17-0119.1>, 2017.
- 435 Allen, J. T., Giammanco, I. M., Kumjian, M. R., Jurgen Punge, H., Zhang, Q., Groenemeijer, P., Kunz, M., and Ortega, K.: Understanding Hail in the Earth System, *Reviews of Geophysics*, 58, 1–49, <https://doi.org/10.1029/2019RG000665>, 2020.
- Angulo-Martínez, M., Beguería, S., Latorre, B., and Fernández-Raga, M.: Comparison of precipitation measurements by OTT Parsivel2 and Thies LPM optical disdrometers, *Hydrology and Earth System Sciences*, 22, 2811–2837, <https://doi.org/10.5194/hess-22-2811-2018>, 2018.
- 440 Battaglia, A., Rustemeier, E., Tokay, A., Blahak, U., and Simmer, C.: PARSIVEL snow observations: A critical assessment, *Journal of Atmospheric and Oceanic Technology*, 27, 333–344, <https://doi.org/10.1175/2009JTECHA1332.1>, 2010.
- Beal, A., Hallak, R., Martins, L. D., Martins, J. A., Biz, G., Rudke, A. P., and Tarley, C. R.: Climatology of hail in the triple border Paraná, Santa Catarina (Brazil) and Argentina, *Atmospheric Research*, 234, 104 747, <https://doi.org/10.1016/j.atmosres.2019.104747>, 2020.
- Blanchard, D. C. and Spencer, A. T.: Experiments on the Generation of Raindrop-Size Distributions by Drop Breakup, *Journal of the*
- 445 *Atmospheric Sciences*, 27, 101–108, [https://doi.org/10.1175/1520-0469\(1970\)027<0101:EOTGOR>2.0.CO;2](https://doi.org/10.1175/1520-0469(1970)027<0101:EOTGOR>2.0.CO;2), 1970.
- Brimelow, J. C., Burrows, W. R., and Hanesiak, J. M.: The changing hail threat over North America in response to anthropogenic climate change, *Nature Climate Change*, <https://doi.org/10.1038/nclimate3321>, 2017.
- Bringi, V. N. and Chandrasekar, V.: *Polarimetric Doppler Weather Radar: Principles and Applications*, Cambridge University Press, <https://books.google.com.pe/books?id=KvJvfP9t5Y8C>, 2001.
- 450 Brooks, H. E.: Severe thunderstorms and climate change, <https://doi.org/10.1016/j.atmosres.2012.04.002>, 2013.
- Changnon, S. A.: Increasing major hail losses in the U.S., *Climatic Change*, 96, 161–166, <https://doi.org/10.1007/s10584-009-9597-z>, 2009.
- Chavez, S. P., Silva, Y., and Barros, A. P.: High-Elevation Monsoon Precipitation Processes in the Central Andes of Peru, *Journal of Geophysical Research: Atmospheres*, 125, 0–3, <https://doi.org/10.1029/2020JD032947>, 2020.
- Del Castillo-Velarde, C., Kumar, S., Valdivia-Prado, J. M., Moya-Álvarez, A. S., Flores-Rojas, J. L., Villalobos-Puma, E., Martínez-Castro,
- 455 D., and Silva-Vidal, Y.: Evaluation of GPM Dual-Frequency Precipitation Radar Algorithms to Estimate Drop Size Distribution Parameters, Using Ground-Based Measurement over the Central Andes of Peru, *Earth Systems and Environment*, <https://doi.org/10.1007/s41748-021-00242-5>, 2021.
- Dennis, E. J. and Kumjian, M. R.: The impact of vertical wind shear on hail growth in simulated supercells, *Journal of the Atmospheric Sciences*, <https://doi.org/10.1175/JAS-D-16-0066.1>, 2017.
- 460 Dessens, J., Berthet, C., and Sanchez, J. L.: Change in hailstone size distributions with an increase in the melting level height, *Atmospheric Research*, <https://doi.org/10.1016/j.atmosres.2014.07.004>, 2015.
- Diaz, H. F. and Murnane, R. J.: *Climate Extremes and Society*, Cambridge University Press, <https://doi.org/10.1017/CBO9780511535840>, 2008.
- Diffenbaugh, N. S., Scherer, M., and Trapp, R. J.: Robust increases in severe thunderstorm environments in response to greenhouse forcing,
- 465 *Proceedings of the National Academy of Sciences of the United States of America*, <https://doi.org/10.1073/pnas.1307758110>, 2013.



- Doviak, R. J., Zrníc, D. S., and Sirmans, D. S.: Doppler Weather Radar, *Proceedings of the IEEE*, 67, 1522–1553, <https://doi.org/10.1109/PROC.1979.11511>, 1979.
- Flores-Rojas, J. L., Silva, Y., Suárez-Salas, L., Estevan, R., Valdivia-Prado, J., Saavedra, M., Giraldez, L., Piñas-Laura, M., Scipión, D., Milla, M., Kumar, S., and Martínez-Castro, D.: Analysis of Extreme Meteorological Events in the Central Andes of Peru Using a Set of  
470 Specialized Instruments, *Atmosphere*, 12, 408, <https://doi.org/10.3390/atmos12030408>, 2021.
- Friedrich, K., Higgins, S., Masters, F. J., and Lopez, C. R.: Articulating and Stationary PARSIVEL Disdrometer Measurements in Conditions with Strong Winds and Heavy Rainfall, *Journal of Atmospheric and Oceanic Technology*, 30, 2063–2080, <https://doi.org/10.1175/JTECH-D-12-00254.1>, 2013a.
- Friedrich, K., Kalina, E. A., Masters, F. J., and Lopez, C. R.: Drop-Size Distributions in Thunderstorms Measured by Optical Disdrometers  
475 during VORTEX2, *Monthly Weather Review*, 141, 1182–1203, <https://doi.org/10.1175/MWR-D-12-00116.1>, 2013b.
- Giráldez, L., Silva, Y., Zubieta, R., and Sulca, J.: Change of the Rainfall Seasonality Over Central Peruvian Andes: Onset, End, Duration and Its Relationship With Large-Scale Atmospheric Circulation, *Climate*, 8, 23, <https://doi.org/10.3390/cli8020023>, 2020.
- Hoogewind, K. A., Baldwin, M. E., and Trapp, R. J.: The impact of climate change on hazardous convective weather in the United States: Insight from high-resolution dynamical downscaling, *Journal of Climate*, <https://doi.org/10.1175/JCLI-D-16-0885.1>, 2017.
- 480 Houze, R. A.: Cloud dynamics, *Cloud dynamics*, p. 573, [https://doi.org/10.1016/0377-0265\(87\)90017-0](https://doi.org/10.1016/0377-0265(87)90017-0), 1993.
- Jaffrain, J. and Berne, A.: Experimental Quantification of the Sampling Uncertainty Associated with Measurements from PARSIVEL Disdrometers, *Journal of Hydrometeorology*, 12, 352–370, <https://doi.org/10.1175/2010JHM1244.1>, 2011.
- Jaffrain, J. and Berne, A.: Quantification of the small-scale spatial structure of the raindrop size distribution from a network of disdrometers, *Journal of Applied Meteorology and Climatology*, 51, 941–953, <https://doi.org/10.1175/JAMC-D-11-0136.1>, 2012.
- 485 Jaffrain, J., Studzinski, A., and Berne, A.: A network of disdrometers to quantify the small-scale variability of the raindrop size distribution, *Water Resources Research*, 47, 1–8, <https://doi.org/10.1029/2010WR009872>, 2011.
- Jia, X., Liu, Y., Ding, D., Ma, X., Chen, Y., Bi, K., Tian, P., Lu, C., and Quan, J.: Combining disdrometer, microscopic photography, and cloud radar to study distributions of hydrometeor types, size and fall velocity, *Atmospheric Research*, 228, 176–185, <https://doi.org/10.1016/j.atmosres.2019.05.025>, 2019.
- 490 Knight, C. A. and Knight, N. C.: Hailstorms, in: *Severe Convective Storms*, pp. 223–254, American Meteorological Society, Boston, MA, [https://doi.org/10.1007/978-1-935704-06-5\\_6](https://doi.org/10.1007/978-1-935704-06-5_6), 2001.
- Knight, N. C.: The Climatology of Hailstone Embryos, *Journal of Applied Meteorology*, 20, 750–755, [https://doi.org/10.1175/1520-0450\(1981\)020<0750:TCOHE>2.0.CO;2](https://doi.org/10.1175/1520-0450(1981)020<0750:TCOHE>2.0.CO;2), 1981.
- Kumar, S., Del Castillo-Velarde, C., Prado, J. M., Rojas, J. L. F., Gutierrez, S. M., Alvarez, A. S., Martine-Castro, D., and Silva, Y.: Rainfall  
495 characteristics in the mantaro basin over tropical andes from a vertically pointed profile rain radar and in-situ field campaign, *Atmosphere*, 11, <https://doi.org/10.3390/atmos11030248>, 2020.
- Kunz, M., Sander, J., and Kottmeier, C.: Recent trends of thunderstorm and hailstorm frequency and their relation to atmospheric characteristics in southwest Germany, *International Journal of Climatology*, <https://doi.org/10.1002/joc.1865>, 2009.
- Kunz, M., Blahak, U., Handwerker, J., Schmidberger, M., Punge, H. J., Mohr, S., Fluck, E., and Bedka, K. M.: The severe hailstorm in southwest Germany on 28 July 2013: characteristics, impacts and meteorological conditions, *Quarterly Journal of the Royal Meteorological Society*, <https://doi.org/10.1002/qj.3197>, 2018.
- 500 Lamb, D. and Verlinde, J.: *Physics and Chemistry of Clouds*, Cambridge University Press, <https://doi.org/10.1017/CBO9780511976377>, 2011.



- Löffler-Mang, M. and Joss, J.: An optical disdrometer for measuring size and velocity of hydrometeors, *Journal of Atmospheric and Oceanic Technology*, 17, 130–139, [https://doi.org/10.1175/1520-0426\(2000\)017<0130:AODFMS>2.0.CO;2](https://doi.org/10.1175/1520-0426(2000)017<0130:AODFMS>2.0.CO;2), 2000.
- Ludlam, F. H.: *The hail problem*, Unione nazionale antigrandine, 1958.
- Mahoney, K., Alexander, M. A., Thompson, G., Barsugli, J. J., and Scott, J. D.: Changes in hail and flood risk in high-resolution simulations over Colorado’s mountains, *Nature Climate Change*, <https://doi.org/10.1038/nclimate1344>, 2012.
- Martins, J. A., Brand, V. S., Capucim, M. N., Felix, R. R., Martins, L. D., Freitas, E. D., Gonçalves, F. L., Hallak, R., Dias, M. A. F. S., and Cecil, D. J.: Climatology of destructive hailstorms in Brazil, *Atmospheric Research*, 184, 126–138, <https://doi.org/10.1016/j.atmosres.2016.10.012>, 2017.
- Matthews, J. H. and Mason, B. J.: Electrification produced by the rupture of large water drops in an electric field, *Quarterly Journal of the Royal Meteorological Society*, 90, 275–286, <https://doi.org/10.1002/qj.49709038506>, 1964.
- Mezher, R. N., Doyle, M., and Barros, V.: Climatology of hail in Argentina, *Atmospheric Research*, 114–115, 70–82, <https://doi.org/10.1016/j.atmosres.2012.05.020>, 2012.
- Park, S. G., Kim, H. L., Ham, Y. W., and Jung, S. H.: Comparative evaluation of the OTT PARSIVEL2 using a collocated two-dimensional video disdrometer, *Journal of Atmospheric and Oceanic Technology*, 34, 2059–2082, <https://doi.org/10.1175/JTECH-D-16-0256.1>, 2017.
- Peters, G., Fischer, B., and Clemens, M.: Rain attenuation of radar echoes considering finite-range resolution and using drop size distributions, *Journal of Atmospheric and Oceanic Technology*, 27, 829–842, <https://doi.org/10.1175/2009JTECHA1342.1>, 2010.
- Prein, A. F. and Heymsfield, A. J.: Increased melting level height impacts surface precipitation phase and intensity, *Nature Climate Change*, <https://doi.org/10.1038/s41558-020-0825-x>, 2020.
- Prein, A. F. and Holland, G. J.: Global estimates of damaging hail hazard, *Weather and Climate Extremes*, 22, 10–23, <https://doi.org/10.1016/j.wace.2018.10.004>, 2018.
- Prieto, R., Gimeno, L., García, R., Herrera, R., Hernández, E., and Ribera, P.: Interannual variability of hail-days in the Andes region since 1885, *Earth and Planetary Science Letters*, 171, 503–509, [https://doi.org/10.1016/S0012-821X\(99\)00170-3](https://doi.org/10.1016/S0012-821X(99)00170-3), 1999.
- Pruppacher, H. and Klett, J.: *Microphysics of Clouds and Precipitation*, vol. 18 of *Atmospheric and Oceanographic Sciences Library*, Springer Netherlands, Dordrecht, 2 edn., <https://doi.org/10.1007/978-0-306-48100-0>, 2010.
- Púčik, T., Castellano, C., Groenemeijer, P., Kühne, T., Rädler, A. T., Antonescu, B., and Faust, E.: Large hail incidence and its economic and societal impacts across Europe, *Monthly Weather Review*, <https://doi.org/10.1175/MWR-D-19-0204.1>, 2019.
- Rasmussen, K. L., Prein, A. F., Rasmussen, R. M., Ikeda, K., and Liu, C.: Changes in the convective population and thermodynamic environments in convection-permitting regional climate simulations over the United States, *Climate Dynamics*, <https://doi.org/10.1007/s00382-017-4000-7>, 2020.
- Rasmussen, R. M. and Heymsfield, A. J.: Melting and Shedding of Graupel and Hail. Part II: Sensitivity Study, *Journal of the Atmospheric Sciences*, 44, 2764–2782, [https://doi.org/10.1175/1520-0469\(1987\)044<2764:MASOGA>2.0.CO;2](https://doi.org/10.1175/1520-0469(1987)044<2764:MASOGA>2.0.CO;2), 1987.
- Raupach, T. H. and Berne, A.: Correction of raindrop size distributions measured by Parsivel disdrometers, using a two-dimensional video disdrometer as a reference, *Atmospheric Measurement Techniques*, 8, 343–365, <https://doi.org/10.5194/amt-8-343-2015>, 2015.
- Raupach, T. H., Martius, O., Allen, J. T., Kunz, M., Lasher-Trapp, S., Mohr, S., Rasmussen, K. L., Trapp, R. J., and Zhang, Q.: The effects of climate change on hailstorms, *Nature Reviews Earth and Environment*, 2, 213–226, <https://doi.org/10.1038/s43017-020-00133-9>, 2021.
- Silva, Y., Takahashi, K., and Chávez, R.: Dry and wet rainy seasons in the Mantaro river basin (Central Peruvian Andes), *Advances in Geosciences*, 14, 261–264, <https://doi.org/10.5194/adgeo-14-261-2008>, 2008.





- Tokay, A., Wolff, D. B., and Petersen, W. A.: Evaluation of the new version of the laser-optical disdrometer, OTT parsivel, *Journal of Atmospheric and Oceanic Technology*, 31, 1276–1288, <https://doi.org/10.1175/JTECH-D-13-00174.1>, 2014.
- Tokay, A., D'Adderio, L. P., Wolff, D. B., and Petersen, W. A.: A field study of pixel-scale variability of raindrop size distribution in the Mid-Atlantic region, *Journal of Hydrometeorology*, 17, 1855–1868, <https://doi.org/10.1175/JHM-D-15-0159.1>, 2016.
- 545 Trapp, R. J., Diffenbaugh, N. S., Brooks, H. E., Baldwin, M. E., Robinson, E. D., and Pal, J. S.: Changes in severe thunderstorm environment frequency during the 21st century caused by anthropogenically enhanced global radiative forcing, *Proceedings of the National Academy of Sciences of the United States of America*, <https://doi.org/10.1073/pnas.0705494104>, 2007.
- Trapp, R. J., Hoogewind, K. A., and Lasher-Trapp, S.: Future changes in hail occurrence in the United States determined through convection-permitting dynamical downscaling, *Journal of Climate*, <https://doi.org/10.1175/JCLI-D-18-0740.1>, 2019.
- 550 Valdivia, J. and Silva, Y.: Estadística de ocurrencia de tormentas en el Observatorio de Huancayo, Tech. Rep. October, Insitituto Geofísico del Perú, <https://doi.org/10.13140/RG.2.2.22792.37121>, 2016.
- Valdivia, J. M., Contreras, K., Martinez-Castro, D., Villalobos-Puma, E., Suarez-Salas, L. F., and Silva, Y.: Dataset on raindrop size distribution, raindrop fall velocity and precipitation data measured by disdrometers and rain gauges over Peruvian central Andes (12.0°S), *Data in Brief*, 29, 105 215, <https://doi.org/10.1016/j.dib.2020.105215>, 2020a.
- 555 Valdivia, J. M., Scipión, D. E., Milla, M., and Silva, Y.: Multi-Instrument Rainfall-Rate Estimation in the Peruvian Central Andes, *Journal of Atmospheric and Oceanic Technology*, 37, 1811–1826, <https://doi.org/10.1175/jtech-d-19-0105.1>, 2020b.
- Villalobos-Puma, E., Martinez-Castro, D., Flores-Rojas, J. L., Saavedra-Huanca, M., and Silva-Vidal, Y.: Diurnal Cycle of Raindrops Size Distribution in a Valley of the Peruvian Central Andes, *Atmosphere*, 11, 38, <https://doi.org/10.3390/atmos11010038>, 2019.
- Villermaux, E. and Bossa, B.: Single-drop fragmentation determines size distribution of raindrops, *Nature Physics*, 5, 697, <https://doi.org/10.1038/nphys1340>, 2009.
- 560 Weisman, M. L. and Klemp, J. B.: The structure and classification of numerically simulated convective storms in directionally varying wind shears., *Monthly Weather Review*, [https://doi.org/10.1175/1520-0493\(1984\)112<2479:TSACON>2.0.CO;2](https://doi.org/10.1175/1520-0493(1984)112<2479:TSACON>2.0.CO;2), 1984.
- Williams, C. R., Ecklund, W. L., and Gage, K. S.: Classification of Precipitating Clouds in the Tropics Using 915-MHz Wind Profilers, [https://doi.org/10.1175/1520-0426\(1995\)012<0996:COPCIT>2.0.CO;2](https://doi.org/10.1175/1520-0426(1995)012<0996:COPCIT>2.0.CO;2), 1995.
- 565 Williams, C. R., Maahn, M., Hardin, J. C., and de Boer, G.: Clutter mitigation, multiple peaks, and high-order spectral moments in 35 GHz vertically pointing radar velocity spectra, *Atmospheric Measurement Techniques*, 11, 4963–4980, <https://doi.org/10.5194/amt-11-4963-2018>, 2018.
- WMO, W. M. O.: *International Cloud Atlas: Manual on the Observation of Clouds and Other Meteors.*, 2017.
- Xie, B., Zhang, Q., and Wang, Y.: Trends in hail in China during 1960-2005, *Geophysical Research Letters*, <https://doi.org/10.1029/2008GL034067>, 2008.
- 570